

Numerical algorithms for an inverse problem of corrosion detection

Giulia Deolmi¹, Fabio Marcuzzi¹, Sergio Marinetti², Silvia Poles³

¹*Department of Pure and Applied Mathematics, University of Padova, Italy*
gdeolmi@math.unipd.it, marcuzzi@math.unipd.it

²*Istituto per le Tecnologie della Costruzione, Consiglio Nazionale delle Ricerche*
sergio.marinetti@itc.cnr.it

³*EnginSoft S.p.a.*
s.poles@enginsoft.it

Communicated by Giorgio Fotia

Abstract

This paper describes a numerical strategy for the detection of hidden corrosion in an internal, unobservable surface of a material object, whose geometry and material properties are known. Since the corrosion is not directly measurable, it is estimated using a nondestructive infrared thermographic inspection. The a priori knowledge about the material object allows us to use a physical-mathematical model to support the estimate. Given a suitable parametrization of the depth of the real corroded profile, the numerical algorithm performs a nonlinear estimate of the corroded model domain parameters, adopting a predictor-corrector scheme.

Keywords: Inverse problem, finite element model, corrosion detection.

AMS Subject Classification: 05A16, 65N38, 78M50

1. Introduction

In this paper we solve numerically an inverse problem of corrosion detection in an unobservable surface of a metal slab, whose thickness and thermo physical properties are known. Since the corrosion is not directly measurable, we estimate it using a nondestructive infrared thermographic inspection. The a priori knowledge about the material object allows us to use a physical-mathematical model to support the estimate. Given a suitable discretization of the corrosion geometric profile and starting from the reference (sound) domain, the mathematical problem consists in estimating the corrosion depth at each interval of the discrete profile.

Pulsed infrared thermography becomes practical in detecting hidden

Received 2010 09 29, in final form 2011 02 22

Published 2011 03 12

corrosion when induced temperature signals are high enough, even if they exist for short time intervals. The 1D approach models only the depth dimension and it therefore assumes that transient thermal events occur simultaneously in sound and corroded areas of the surface: the defects have to be very large so that the boundary heat diffusion effect can be neglected in their center. In such a case an analytical approach is possible. However, when dealing with small defects, the lateral heat diffusion is no longer negligible and must be taken into account (2D and 3D cases) [1]. This paper is focused on the 2D problem: a Finite Element (FE) model is used in an optimization loop to solve the inverse heat transfer problem.

In the framework of the two-dimensional (2D) approach, it has been shown that pulse heating is capable of producing high temperature contrasts but absolute temperature signals might be low due to the insufficient amount of total energy injected into the sample. Oppositely, long heating can significantly warm up the tested object but provides lower contrasts over defects [2]. In the literature, different aspects and solution methods for this kind of problems have been studied. In [3,4] the authors consider the time-harmonic case. Uniqueness and stability have been studied in [5–7].

In the numerical model adopted in this paper, the depth of the real corroded profile is approximated by a general piecewise-constant function. Since it can have high gradients in unknown positions, the simplest strategy is to use a uniform small subdivision step. However, this corresponds to a large number of parameters to be estimated, increasing the computational complexity of the estimation problem. Considering also its ill-conditioning, it may ask for prohibitive computing times for a real-time diagnostic instrument. In principle less parameters could be sufficient to have a good approximation of the depth of the real corroded profile, for example where it possesses small gradients. In identification theory using a model of complexity not higher than necessary is a guideline [8]. In the problem at hand, this can be accomplished by using an *adaptive* subdivision of the profile, based on a posteriori indicators, obtained after iterative comparisons between the experimental measurements and the predictions given by a reference adaptive FE model. In [9], two different algorithms were presented to solve the corrosion estimation problem from the experimental data produced by infrared thermography. While the first one (*inner-outer loop algorithm*) estimates the values of parameters using two nested loops, in the second one (*predictor-corrector algorithm*), to reduce computational costs, the adaptation of the parametrization is done by a linear predictor step, while parameter estimation is done in the nonlinear corrector step. In this paper a novel formulation of the prediction step is presented, theoretically supported by Lemma 4.1 and described in section 4.4.

In section 2, the mathematical problem is presented in the general and 2D cases. In section 3 a suitable parametrization is chosen for the discrete inverse problem at hand. The numerical strategy is described in section 4 and tested in section 5.

2. Problem formulation

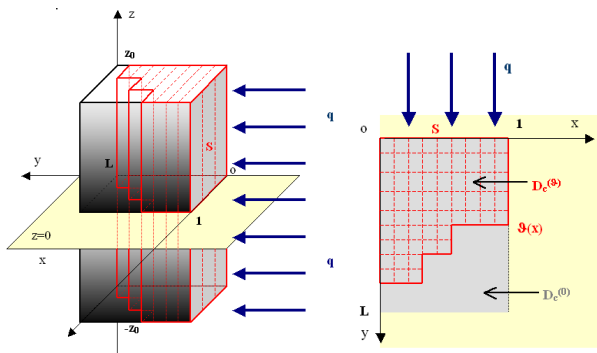


Fig. 1. 3D problem: corroded piece of material (red), absorbs the heat flux \mathbf{q} (left); 2D reduction, dealing with its section over $z = 0$ (right).

Suppose to deal with a metal slab, $D_c^{(0)}$, whose thickness and thermo physical properties are known, and to interact only with one face S , which is provided with n_y temperature sensors. A nondestructive test is used, consisting of an infrared thermographic inspection: in the time interval $[0, t_f]$, $t_f > 0$, S is heated with a thermal flash $\mathbf{q}(t)$ and experimental temperatures are collected. Suppose that the material surface, excluding S , is adiabatic: there is no heat exchange with the outside environment (cfr. Remark 2.1).

The underlying mathematical model is based on solving the heat equation on the corroded domain.

More precisely, let $D_c^{(0)} = [0, 1] \times [0, L] \times [-z_0, z_0]$ be the *reference uncorroded (sound) domain* (Figure 1 left), $S := \{(x, 0, z), x \in [0, 1], z \in [-z_0, z_0]\}$ and solve the following linear heat conduction problem

$$(1) \quad \begin{cases} \rho C \frac{\partial}{\partial t} T^{(0)} = k \Delta T^{(0)}, & \text{in } D_c^{(0)} \times [0, t_f] \\ k \nabla T^{(0)} \cdot \mathbf{n}_S = q(t), & \text{on } S \times [0, t_f] \\ k \nabla T^{(0)} \cdot \mathbf{n} = 0, & \text{on } \delta D_c^{(0)} / S \times [0, t_f] \\ T^{(0)}(0, \cdot) = T_0(\cdot), & \text{in } D_c^{(0)}. \end{cases}$$

ρC is the heat capacity of the material, k is its thermal conductivity, and \mathbf{n}_S and \mathbf{n} are respectively the outward normal to S and $\delta D_c^{(0)}/S$. Suppose to know ρC , k and the heat flux $\mathbf{q}(t) = -q(t)\mathbf{n}_S$, which is assumed to be approximately a Dirac impulse in time, centered in $t = 0$, and constant over S . In section 5 the heat flux is modelled by $q(t) = \frac{Wt}{\sigma_q^2} e^{-\frac{\sqrt{t}}{\sigma_q}}$, with $\sigma_q > 0$ sufficiently small to have a narrow pulse and $W > 0$. The initial condition $T_0(\cdot)$ is simply set as a constant temperature over the spatial domain. Observe that (1) is the *reference sound model*. Consider a temporal discretization of $[0, t_f]$, $\{t_0, \dots, t_{N-1}\}$, $t_0 = 0$, $t_{N-1} = t_f$. The experimental data of the sound model are denoted by $T_{uc}^s \in \mathbb{R}^{n_y \times N}$, such that $(T_{uc}^s)_{ij}$ represents the temperature in the i -th sensor at time t_{j-1} . The FE solution of (1) in S n_y nodes is denoted by $T_h^{(0)} \in \mathbb{R}^{n_y \times N}$. More details regarding the FE discretization of the heat equation can be found for example in [10,11]. The quantity

$$\sigma := \left\| T_{uc}^s - T_h^{(0)} \right\|_2$$

is a measure of the goodness of the model.

Consider now the real *corroded domain* $D_c^{(\vartheta)}$ (cfr. the dashed domain in Figure 1), described by a scalar function $\vartheta \in \mathcal{L}^2(S)$. The corresponding PDE over $D_c^{(\vartheta)}$ is the following

$$(2) \quad \begin{cases} \rho C \frac{\partial}{\partial t} T^{(\vartheta)} = k \Delta T^{(\vartheta)}, & \text{in } D_c^{(\vartheta)} \times [0, t_f] \\ k \nabla T^{(\vartheta)} \cdot \mathbf{n}_S = q(t), & \text{on } S \times [0, t_f] \\ k \nabla T^{(\vartheta)} \cdot \mathbf{n} = 0, & \text{on } \delta D_c^{(\vartheta)}/S \times [0, t_f] \\ T^{(\vartheta)}(0, \cdot) = T_0(\cdot), & \text{in } D_c^{(\vartheta)}. \end{cases}$$

Assume that the corrosion does not modify the boundary conditions, but only the geometry of the domain.

Supposing that the temperatures $T^{(\vartheta)}(t, \cdot)|_S$ are known, the *continuous inverse problem* consists in finding a suitable approximation $\bar{\vartheta} \in \mathcal{L}^2(S)$ of the *depth of the real corroded profile* ϑ s.t.

$$(3) \quad \bar{\vartheta} = \arg \min_{f \in \mathcal{L}^2(S)} \int_0^{t_f} \left\| T^{(\vartheta)}(t, \cdot)|_S - T^{(f)}(t, \cdot)|_S \right\|_{\mathcal{L}^2(S)} dt.$$

This non-destructive approach is physically motivated by the fact that, in presence of corrosion, the heat supplied at the surface accessible from the source, S , has less material to diffuse within and the superficial temperature in S remains locally higher for a nontrivial time-interval $[0, t_f]$: a mathematical proof of this property is given in Lemma 4.1.

In the following it is assumed that, if we are able to accurately describe the depth of the real corroded profile, we can describe the thermal response of the corroded system at the same level of accuracy that we do with the uncorroded one (σ). In this way we can distinguish whether a suboptimal estimate of the profile have been reached.

Remark 2.1. The adiabatic hypothesis is usually invoked in thermal Non-Destructive Evaluation when dealing with thin metal slab. Indeed the key parameter is the *Biot number* which is defined as the ratio of the heat transfer resistances inside of and at the surface of a body. The smaller the Biot number the better the approximation of the real thermal process with an adiabatic one. In figure 2, the surface temperature evolutions (analyti-

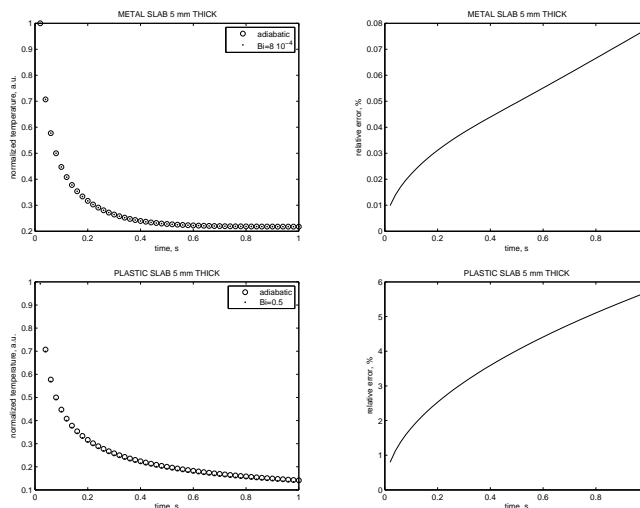


Fig. 2. *First row: metal slab. Left: comparison between surface temperature evolution of a 5 mm thick metal slab in adiabatic and non-adiabatic conditions. Right: Relative error caused by modeling the non-adiabatic process with an adiabatic one. Second row: plastic slab. Left: comparison between surface temperature evolution of a 5 mm thick plastic slab in adiabatic and non-adiabatic conditions. Right: Relative error caused by modeling the non-adiabatic process with an adiabatic one.*

cally computed) for a 5 mm thick slab heated by a Dirac energy pulse in adiabatic and non-adiabatic conditions are shown, for two different materials: metal and plastic. In case of plastic, the Biot number is more than 600 times larger than metal. In this example, the assumption of adiabatic thermal process causes errors in temperature less than 0.1% in case of metal and less than 10% for plastic.

Moreover, in [7] a numerical approach is used to support the consistency

of the adiabatic hypothesis.

2.1. Reduction to a 2D problem

In the following, we assume that the corrosion does not vary along the z -axis, such that (1) and (2) can be restated as 2D problems, considering $S = [0, 1]$ and $D_c^{(0)} = [0, 1] \times [0, L]$ (Figure 1 right). Thus we can describe analytically the corroded region in the following way:

$$D_c^{(\vartheta)} := \{(x, y) \text{ s.t. } x \in [0, 1], 0 \leq y \leq L - \vartheta(x)\},$$

where $\vartheta(x) : [0, 1] \rightarrow [0, L]$ is a suitable smooth non negative function, s.t. $\vartheta(0) = 0 = \vartheta(1)$, which represents the *the depth of the real corroded profile*.

2.2. Choice of a numerical solution strategy

In [3], under suitable hypothesis, the corrosion estimation problem has been solved analytically: assuming a sinusoidal impulse $q(t)$, using a change of coordinates, (2) is rewritten as a heat equation over the sound domain $D_c^{(0)} \times [0, t_f]$, with its PDE coefficients depending on θ . However, in this paper it is assumed that the heating flux $q(t)$ is approximately a *Dirac pulse heating*. Its use is motivated by higher contrast signal and shorter test duration. Indeed pulse thermography, that is a transient technique, does not require the sample to reach the stationary periodic regime, as in case of an harmonic heating. Since the analytical solution of the corresponding heat equation becomes very difficult, a numerical approach has been adopted. Observe that a discrete restatement of the inverse problem (3) is proper, since we suppose to deal with collected experimental data $T_c^s \in \mathbb{R}^{n_y \times N}$.

3. The discrete inverse problem

To restate (3) as a discrete inverse problem, a particular approximation of the depth of the real corroded profile $\vartheta(x)$ is introduced, choosing a *piecewise constant function* (Figure 1 right).

Consider a subdivision of $[0, 1]$, coincident with a subset of the n_y temperature sensors' locations, with distinct spatial nodes $\{x_i\}_{i=1, \dots, n_\theta}$, $n_\theta \leq n_y$, $x_0 = 0$, $x_{n_\theta} = 1$, and a uniform subdivision of $[0, L]$, with step h_y , $\{y_i\}_{i=0, \dots, n_L}$, $y_0 = 0$, $y_{n_L} = L$. Define

$$\theta_j := \frac{1}{h_c(j)} \int_{x_j}^{x_{j+1}} \vartheta(x) dx \approx L - y_k,$$

for a suitable $k \in \{0, \dots, n_L\}$, $h_c(j) := |x_{j+1} - x_j|$, $j = 1, \dots, n_\theta - 1$.

Consider now the set of functions

$$\mathcal{P} = \left\{ \tilde{\vartheta} \text{ s.t. } \tilde{\vartheta} : [0, 1] \longrightarrow [0, L], \tilde{\vartheta}(x) = \sum_{j=1}^{n_\theta-1} \theta_j \chi_{[x_i, x_{i+1})}(x) \right\},$$

where $\chi_{[x_i, x_{i+1})}(x) = \begin{cases} 1, & x \in [x_i, x_{i+1}) \\ 0, & \text{elsewhere} \end{cases}$ is the characteristic function of $[x_i, x_{i+1})$. The approximated corroded domain is defined as follows

$$D_c^{(\tilde{\theta})} := D_c^{(0)} \setminus \int_0^1 \tilde{\vartheta}(x) dx.$$

Thus $D_c^{(\tilde{\theta})}$ is identified by the vector of parameters $\boldsymbol{\theta} \in \mathbb{R}^{n_\theta-1}$.

Define now the *matrix of prediction errors* $E_\theta := T_c^s - T_h^{(\theta)} \in \mathbb{R}^{n_y \times N}$ where $T_h^{(\theta)} \in \mathbb{R}^{n_y \times N}$ denotes the FE solution at every time discretization point in S' n_y nodes, solving (2) on an approximated corroded domain $D_c^{(\tilde{\theta})}$.

Consider the real valued function $\mathcal{F}_N : \mathbb{R}^{n_\theta-1} \rightarrow \mathbb{R}$,

$$(4) \quad \mathcal{F}_N(\boldsymbol{\theta}) := \frac{1}{N} \sum_{n=1}^N \|E_\theta(\cdot, n)\|_2^2.$$

The discrete version of the inverse problem (3) corresponds to find the optimal $\tilde{\vartheta}^* \in \mathcal{P}$, or equivalently the optimal parameters $\theta_j^*, j = 1, \dots, n_\theta - 1$ such that

$$(5) \quad \boldsymbol{\theta}^* = \arg \min_{\boldsymbol{\theta} \in \mathbb{R}^{n_\theta-1}} \mathcal{F}_N(\boldsymbol{\theta}).$$

Reshaping the matrices, define $\mathbf{e}_\theta, \mathbf{y}, \hat{\mathbf{y}}_\theta \in \mathbb{R}^{n_y N}$ s.t.

$$\begin{aligned} \mathbf{e}_\theta((n-1)n_y + 1 : nn_y) &= E_\theta(:, n), \\ \mathbf{y}((n-1)n_y + 1 : nn_y) &= T_c^s(:, n), \\ \hat{\mathbf{y}}_\theta((n-1)n_y + 1 : nn_y) &= T_h^h(:, n) \end{aligned}$$

$n = 1, \dots, N$. The *sensitivity matrix* $\psi_\theta \in \mathbb{R}^{n_y N \times n_\theta}$ is such that $\psi_\theta(:, i) := \frac{\partial}{\partial \theta_i} \hat{\mathbf{y}}_\theta$, for all $i = 1, \dots, n_\theta$.

Since a piecewise constant approximation of $\vartheta(x)$ is chosen, it must be assumed that every parameter corresponds to a well-defined piece of the real corrosion profile, whose length strictly depends on the local behavior of $\vartheta(x)$. Moreover it is assumed to deal with non overlapping parameters.

In the following the depth of the approximated corroded profile is identified with the real one, which is thus assumed to be piecewise constant. Also numerical experimental data are collected assuming a profile belonging to \mathcal{P} .

4. Adopted numerical approach

Assuming that the real corroded profile is a parametric piecewise constant function, the aim of the numerical algorithm is to estimate the real shape of the domain. It solves the discrete inverse problem (5), using (2) as the underlying direct model, solved in the approximated corroded domain $D_c^{(\hat{\theta})}$.

4.1. Key assumption

Let $\bar{i} \in [1, n_\theta - 1]$, a key assumption in the development of the algorithm is that when at iteration $k + 1$, $k \geq 0$, the estimation algorithm changes the \bar{i} -th component of the estimate $\hat{\theta}^{(k)}(\bar{i})$ to a value $\hat{\theta}^{(k+1)}(\bar{i})$ closer to the real one, leaving unchanged the others, the cost function diminishes monotonically. This property is an immediate consequence of the following physical principle: in $[0, t_f]$, under the same initial and boundary conditions, if $D_{c,1} \subset D_{c,2}$, then temperatures corresponding to the smallest domain $D_{c,1}$ are higher supposing that we are dealing with initial constant temperatures and a thermal flux q which is independent on the space variable. In fact, assuming that $D_c^{(\theta^*)} \subset D_c^{(\hat{\theta}^{(k+1)})} \subset D_c^{(\hat{\theta}^{(k)})}$, it can be deduced that $T_s^c > T_h^{(\hat{\theta}^{(k+1)})} > T_h^{(\hat{\theta}^{(k)})}$ and thus $\mathcal{F}_N(\hat{\theta}^{(k+1)}) < \mathcal{F}_N(\hat{\theta}^{(k)})$. A rigorous proof of this property is given in the following Lemma.

Lemma 4.1. *Consider the heat problems represented in Figure 3, solving*

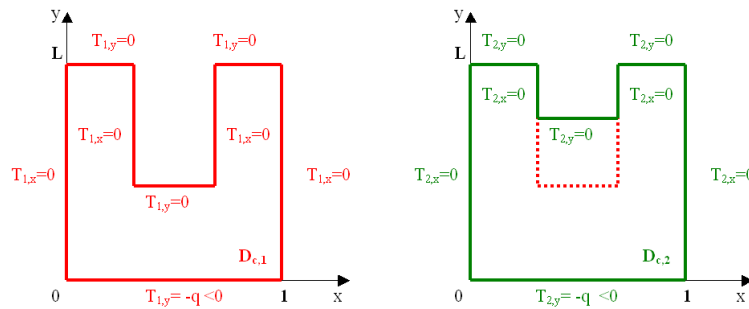


Fig. 3.

the heat equation model

$$(6) \quad \begin{cases} \rho C \frac{\partial}{\partial t} T_i = k \Delta T_i, & \text{in } D_{c,i} \times [0, t_f] \\ k T_{i,y} = -q(t), & \text{on } S \times [0, t_f] \\ k \nabla T_i \cdot \mathbf{n} = 0, & \text{on } \delta D_{c,i} \setminus S \times [0, t_f] \\ T_i(0, x, y) = T_0(x, y), & \text{in } D_{c,i}. \end{cases}$$

where $i = 1, 2$ and $S = [0, 1]$. Moreover define $\frac{\partial T_i}{\partial x} = T_{i,x}$ and $\frac{\partial T_i}{\partial y} = T_{i,y}$. Suppose that temperatures at $t = 0$ are constant in space, $T_0(x, y) = T_0 \in \mathbb{R}$, and that $q(t, x) = q(t) > 0$. Then $T_1(x, y) > T_2(x, y)$ for every $(x, y) \in D_{c,1}$.

Proof. (Lemma 4.1) The proof is a consequence of the *maximum principle for parabolic operators* [12]. To compare temperatures T_1 and T_2 in $D_{c,1}$, it is necessary to collect information about the values taken by T_2 in $D_{c,1}$. To do this, define $v := T_{2,x}$: v satisfies the heat equation $\frac{\partial v}{\partial t} = \Delta v$, under the boundary conditions of Figure 4 (up left), where we have used $v_y = T_{2,xy} = (T_{2,y})_x$. Thus, using the maximum principle for parabolic operators, we know that strictly maximum and minimum values are taken at the boundary, where Dirichlet boundary conditions are applied, or at $t = 0$. Since we assume that T_0 is constant, $v = 0$ at $t = 0$. It follows that

$$T_{2,x}(t, x, y) = v(t, x, y) = 0$$

for every $(t, x, y) \in [0, t_f] \times D_{c,2}$. Moreover define $z := T_{2,y}$: z is a solution of

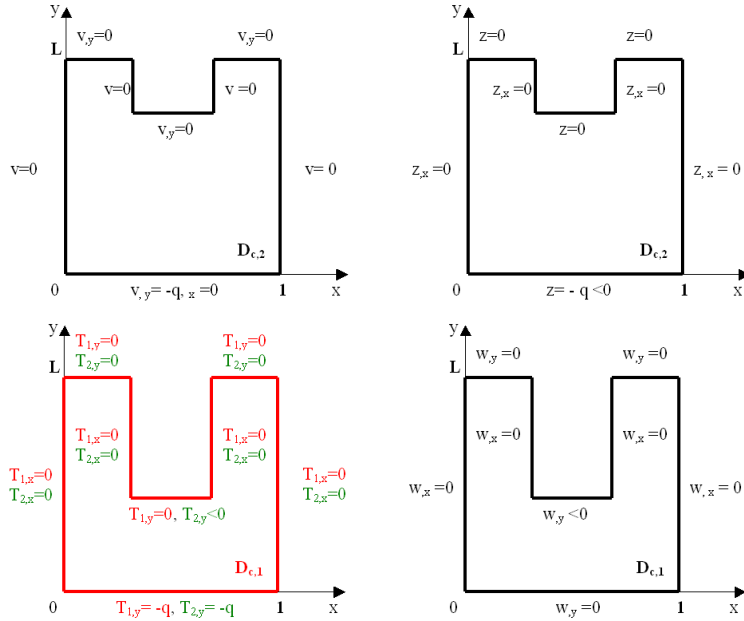


Fig. 4. $v := T_{2,x}$, $z := T_{2,y}$, $w := T_2 - T_1$.

the heat equation $\frac{\partial z}{\partial t} = \Delta z$, under the boundary conditions of Figure 4 (up right), where we have used $z_x = T_{2,yx} = (T_{2,x})_y$. Using again the maximum

principle we conclude that

$$-q(t) \leq T_{2,y}(t, x, y) = z(t, x, y) \leq 0,$$

for every $t \in [0, t_f]$ and (x, y) in the interior of $D_{c,2}$. All this information is summarized in Figure 4 (bottom left). Now we can compare directly T_1 and T_2 over $D_{c,1} \subset D_{c,2}$: define $w := T_2 - T_1$, which solves the heat equation $\frac{\partial w}{\partial t} = \Delta w$, under the boundary conditions of Figure 4 (bottom right). Now we can again apply the maximum principle. Since we suppose that at $t = 0$ $T_2 = T_1$, $w = 0$ in $t = 0$. Moreover if a maximum is taken, then it must be placed on the boundary, where $w_y > 0$ [12]. Since is always $w_y \leq 0$, then a maximum does not exists, thus $w < 0$ over $D_{c,1}$. \square

4.2. Projected damped Gauss-Newton iterations

Given the damping parameter μ^k and $\hat{\theta}^k$, the $k + 1$ -th iteration $\hat{\theta}^{k+1} = \hat{\theta}^k + \mu^k \mathbf{s}^k$, is obtained substituting the standard Newton step

$$\mathcal{F}'_N(\hat{\theta}^k) \mathbf{s}^k = -\mathcal{F}'_N(\hat{\theta}^k)$$

by the Gauss-Newton approximation:

$$\psi_{\hat{\theta}^k} \mathbf{s}^k = \mathbf{e}_{\hat{\theta}^k}.$$

To compute numerically the sensitivity matrix a centered finite difference scheme is needed: this is computationally expensive, since, in order to estimate one single column, two different temperatures predictions must be computed.

The perturbation of different parameters may produce quite similar responses in the simulation data, generating couples of columns in the matrix ψ_θ which are close to linear dependence. In our problem, this is related to the length of the corrosion profile segment corresponding to each parameter. Thus, *the presence of short segments* $h_c(i)$, $i = 1, \dots, n_\theta - 1$, produces, in general, an ill-conditioned matrix ψ_θ . Therefore, the search for a better accuracy in the determination of the depth of the real corroded profile, which means to reduce the size of a few parameters, brings to higher numerical problems, as usually happens solving inverse problems [13,14]. Thus a regularization technique is needed [9].

4.3. Convergence properties of the projected damped Gauss-Newton method

In this section it will be proved that, if the finer parametrization is chosen and the sites of corrosion are known, then the inverse problem of corrosion estimation is well-posed, or equivalently there are no local minima.

Suppose to use the finer parametrization and to know exactly the sites of corrosion $\{\bar{i}_1, \dots, \bar{i}_l\}$ of the real corroded profile θ^* , $\bar{i}_j \in [1, n_y]$. Thus $\mathcal{F}_N(\theta^*) < \mathcal{F}_N(\theta)$ for every $\theta \in \Psi$, where Ψ denotes the set of profiles with corrosion sites $\{\bar{i}_1, \dots, \bar{i}_l\}$:

$$\Psi = \{\theta \in \mathbb{R}^{n_\theta-1} \text{ s.t. } n_\theta = n_y, \theta(j) = 0, \forall j \notin \{\bar{i}_1, \dots, \bar{i}_l\}\}.$$

A local minima $\bar{\theta}$, is a corrosion profile such that $\mathcal{F}_N(\bar{\theta}) < \mathcal{F}_N(\theta)$ for every $\theta \in \Psi_{\bar{\theta}}$, where $\Psi_{\bar{\theta}}$ is the set of Ψ 's profiles perturbed of a quantity δ :

$$\Psi_{\bar{\theta}} = \{\theta \in \Psi, \theta(j) = \bar{\theta}(j) + \delta_j, \forall j \in \{\bar{i}_1, \dots, \bar{i}_l\}, \delta_j \in \{0, h_y, -h_y\}, \delta \neq \mathbf{0}\}.$$

The following Proposition is equivalent to prove that there are no local minima.

Proposition 4.1. *For every $\bar{\theta} \in \Psi$, $\bar{\theta} \neq \theta^*$, there exists at least a sequence of profiles $\{\theta_n\}_n$, $\theta_0 = \bar{\theta}$, $\theta_{n+1} \in \Psi_{\theta_n}$, converging decreasing in $\mathcal{L}^2(\mathbb{R}^{n_\theta-1})$ to the real corrosion profile θ^* , such that $\mathcal{F}_N(\theta_n) \downarrow \mathcal{F}_N(\theta^*)$.*

First of all we demonstrate the following Lemma.

Lemma 4.2. *Given $\{\bar{i}_1, \dots, \bar{i}_l\}$, for every $\bar{\theta} \in \Psi$, $\bar{\theta} \neq \theta^*$, and for every $k \in [1, l]$ such that $\theta^*(i_k) \neq \bar{\theta}(i_k)$, define*

$$(7) \quad \theta^{*,k}(j) := \begin{cases} \bar{\theta}(j), & j \neq \bar{i}_k \\ \theta^*(j), & j = \bar{i}_k \end{cases},$$

$j = 1, \dots, n_\theta - 1$. Thus for every $\bar{\theta} \in \Psi$ there exists at least a sequence of profiles $\{\theta_n\}_n$, $\theta_0 = \bar{\theta}$, $\theta_{n+1} \in \Psi_{\theta_n}$, converging decreasing in $\mathcal{L}^2(\mathbb{R}^{n_\theta-1})$ to $\theta^{*,k}$: $\mathcal{F}_N(\theta_n) \downarrow \mathcal{F}_N(\theta^{*,k})$.

Proof. (Lemma 4.2)

We indicate with $T_c^{s,k}$ temperatures corresponding to $\theta^{*,k}$.

Let $r \in \mathbb{Z}$ such that $\bar{\theta}(\bar{i}_k) - \theta^{*,k}(\bar{i}_k) = rh_y \neq 0$ by hypothesis.

Suppose that $r > 0$: consider the following converging sequence

$$(8) \quad \theta_n(j) := \begin{cases} \bar{\theta}(j), & j \neq \bar{i}_k \\ \bar{\theta}(j) - nh_y, & j = \bar{i}_k \end{cases},$$

for $n = 0, \dots, r$, $\theta_r = \theta^{*,k}$ by construction, and $\theta_s := \theta_r$, $s \geq n$. An example is sketched in Figure 5 (left). By definition $\theta_0(\bar{i}_k) > \dots > \theta_j(\bar{i}_k) > \theta_{j+1}(\bar{i}_k) > \dots > \theta^{*,k}(\bar{i}_k)$, or equivalently $D_c^{(\theta_0)} \subset \dots \subset D_c^{(\theta_j)} \subset \dots \subset D_c^{(\theta^{*,k})}$. Thus the underlying heat equation operator tells us that temperatures corresponding to θ_j are greater than those corresponding to

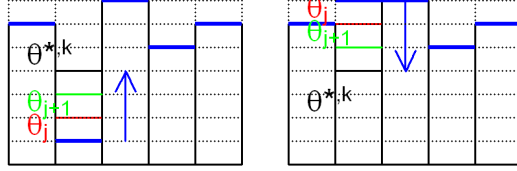


Fig. 5. Converging sequence (8) (left) and (9) (right): in blue $\bar{\theta}(\bar{i}_k)$, in black the optimal profile $\theta^{*,k}(\bar{i}_k)$, in red $\theta_j(\bar{i}_k)$ and in green $\theta_{j+1}(\bar{i}_k)$.

θ_{j+1} , and they are both greater than $T_c^{s,k}$, applying Lemma 4.1. Thus $\mathcal{F}_N(\theta_0) > \dots > \mathcal{F}_N(\theta^{*,k})$.

Finally observe that if $r < 0$, the proof is analogous considering

$$(9) \quad \theta_n(j) := \begin{cases} \bar{\theta}(j), & j \neq \bar{i}_k \\ \bar{\theta}(j) + nh_y, & j = \bar{i}_k \end{cases}$$

for $n = 0, \dots, |r|$ instead of (8) (Figure 5 (right)). \square

Proof. (Proposition 4.1).

We use the above Lemma 4.2. In fact, suppose that the corrosion sites are $\{\bar{i}_1, \dots, \bar{i}_l\}$. Thus we can construct the sequence $\{\theta_n\}_n$ in the following way. Suppose that $k_1 \in [1, l]$ is the first index s.t. $\bar{\theta}(\bar{i}_{k_1}) - \theta^*(\bar{i}_{k_1}) = r_1 h_y$, $r_1 \in \mathbb{Z} \setminus \{0\}$. Thus

$$(10) \quad \theta_n(j) := \begin{cases} \bar{\theta}(j), & j \in [1, n\theta - 1] \setminus \{\bar{i}_{k_1}\} \\ \bar{\theta}(j) + nh_y, & j = \bar{i}_{k_1}, r_1 < 0 \\ \bar{\theta}(j) - nh_y, & j = \bar{i}_{k_1}, r_1 > 0 \end{cases}$$

for $n = 0, \dots, |r_1|$. Using Lemma 4.2 we know that $\mathcal{F}_N(\theta_0) > \mathcal{F}_N(\theta_1) > \dots > \mathcal{F}_N(\theta_{|r_1|})$ and by construction

$$\theta_{|r_1|}(j) = \begin{cases} \bar{\theta}(j), & j \in [1, n\theta - 1] \setminus \{\bar{i}_{k_1}\} \\ \theta^*(j), & j = \bar{i}_{k_1} \end{cases}.$$

Now we choose the second index $k_2 \in [1, l]$ s.t. $\bar{\theta}(\bar{i}_{k_2}) - \theta^*(\bar{i}_{k_2}) = r_2 h_y$, $r_2 \in \mathbb{Z} \setminus \{0\}$ and define $\theta_{|r_1|+1}, \dots, \theta_{|r_1|+|r_2|}$, using (10), replacing r_1 with r_2 and k_1 with k_2 . Using Lemma 4.2 we know that $\mathcal{F}_N(\theta_{|r_1|}) > \mathcal{F}_N(\theta_{|r_1|+1}) > \dots > \mathcal{F}_N(\theta_{|r_2|})$ and by construction

$$\theta_{|r_2|}(j) = \begin{cases} \bar{\theta}(j), & j \in [1, n\theta - 1] \setminus \{\bar{i}_{k_1}, \bar{i}_{k_2}\} \\ \theta^*(j), & j \in \{\bar{i}_{k_1}, \bar{i}_{k_2}\} \end{cases}.$$

This idea can be repeated for every $k \in [1, l]$ s.t. $\bar{\theta}(\bar{i}_k) - \theta^*(\bar{i}_k) \neq 0$. Finally we obtain the desired decreasing sequence $\{\theta_n\}_n$, converging in $\mathcal{L}^2(\mathbb{R}^{n_\theta-1})$ to the real profile θ^* , s.t. $\mathcal{F}_N(\theta_n) \downarrow \mathcal{F}_N(\theta^*)$. \square

4.4. Predictor-Corrector algorithm

As demonstrated in the previous section, the problem is well-posed, if the finer discretization is used and the sites of corrosion are known. Unfortunately the last ones are unknown and using the finer discretization could be very expensive. Thus the practically intrinsic ill-posedness of the inverse problem of corrosion detection, is mainly due to its *adaptive formulation*, which is necessary to reduce the computational cost. In this paper the adaptive parametrization is determined starting from an initial subdivision of the corrosion profile with quite large $h_c(i)$, $i = 1, \dots, n_\theta - 1$ values. According to a suitable *a posteriori indicator*, the algorithm decides where eventually to refine locally the subdivision of the corrosion profile. The refinement operation corresponds to a bisection of the indicated segments, with a consequent increase in the number of segments and, therefore, of parameters of the model. This is iteratively made until the comparison between the actual value of the cost function and the reference value, previously obtained for the sound (uncorroded) system, shows that the model describes the experimental data in an optimal way. As in [9], the *a posteriori indicator* is based upon parameter estimates, obtained at previous iterations. In general these values are accurate only when the parameterization is good, thus they are not always reliable estimates of the corrosion depth; otherwise they are reliable indicators of the *regions* where the corrosion exists. Note that the accuracy of this localization is disturbed by the strong diffusive character of the heat conduction process.

It is assumed to use as initial point the null corrosion profile over a chosen coarse subdivision of S , $\{x_1^0, \dots, x_{n_\theta}^0\}$, $x_1^0 = 0$, $x_{n_\theta}^0 = 1$. Observe that this assumption is motivated by the physical problem: first of all it is important to understand if the material is sound. If not, it is meaningful to adopt a proper research strategy.

4.4.1. Inner-Outer loop algorithm

Given two estimates of θ^* , $\hat{\theta}^{l-1} \in \mathbb{R}^{n_\theta^{l-1}}$ and $\hat{\theta}^l \in \mathbb{R}^{n_\theta^l}$, if there exists at least one $j \in [1, n_\theta^l - 1]$ such that $\theta^l(j) > \theta^{l-1}(j)$, Θ is defined as the set of all indexes j satisfying this property. Otherwise, Θ is the set of j such that $\theta^l(j) > 0$. The new iteration $\hat{\theta}^{l+1}$ is obtained bisecting every segment $[x_j^l, x_{j+1}^l]$ of the l -th subdivision of S , such that $j \in \Theta$. Then, in the inner loop, the projected damped Gauss-Newton method is applied with respect

to the refined subdivision. This method in general converges, but it is slow, due to the computational cost of two nested loops. In fact while the outer loop adapts the parametrization, the inner one estimates model parameters' values for the current refinement level of $[0, 1]$. Moreover this strategy tends to over-refine S .

4.4.2. Formulation of the predictor-corrector algorithm

The high computational cost of the inner-outer loop algorithm has motivated the research of a smarter algorithm: the idea is to reorganize it in a predictor-corrector form [9]. Observe that, since it is assumed to start from the null corrosion profile $\hat{\theta}^0$ it is known that, if the material is corroded, we are underestimating its corrosion profile. The idea is to try to build a sequence of estimated corroded domains, $\{\hat{\theta}^l\}$, $l \geq 0$, avoiding huge overestimations of $\hat{\theta}^*$. In fact in practice small overestimations are usually allowed and preferred to underestimations. To limit progressive refinements and to obtain a better conditioned matrix ψ_θ , two estimators are used: the \mathcal{L}^2 norm and the mean of the prediction error \mathbf{e}_θ respectively. While the norm is a measure of the distance between $\hat{\theta}^l$ and $\hat{\theta}^*$, the mean permits to understand if $\hat{\theta}^l$ is a big overestimate of the profile. In fact, using Lemma 4.1, it is known that a local big overestimate corresponds to local negative values of the prediction error, whose absolute values are big too. More precisely, the predictor step works as follows: given $\Lambda = \emptyset$, which represents the set of parameters to be estimated in the corrector step, given a fixed scalar perturbation $\delta > 0$ and two suitable thresholds α_η , $\alpha_\nu > 0$, substitute the outer loop with the *linear predictor step*. Given $\hat{\theta}^l \in \mathbb{R}^{n_\theta^l-1}$ and the l -th subdivision of S , $\{x_1^l, \dots, x_{n_\theta^l}^l\}$, for every $i \in [1, n_\theta^l - 1]$, consider the perturbed parameter

$$(11) \quad \hat{\theta}_{\delta,i}^l := \begin{cases} \hat{\theta}^l(k) + \delta, & \text{if } k = i \\ \hat{\theta}^l(k), & \text{elsewhere} \end{cases}$$

and compute the corresponding prediction error $\mathbf{E}_{\hat{\theta}_{\delta,i}^l} \in \mathbb{R}^{n_\theta^l \times N}$. Then for all $j \in [1, n_\theta^l]$, $\eta_\delta^l(i, j)$ and $\nu_\delta^l(i, j)$ are computed, the norm and the temporal mean of $\mathbf{E}_{\hat{\theta}_{\delta,i}^l}(j, :)$ respectively.

Given $\eta_\delta^l, \nu_\delta^l \in \mathbb{R}^{n_\theta^l-1 \times n_\theta^l}$, the algorithm proceeds as follows: initialize $\{x_1^{l+1}, \dots, x_{n_\theta^{l+1}}^{l+1}\} = \{x_1^l, \dots, x_{n_\theta^l}^l\}$. Given $I := [1, n_\theta^l - 1]$, for all $i \in I$

- if the perturbation $\hat{\theta}_{\delta,i}^l$ improves significantly the cost function, or

equivalently if $\eta_\delta^l(i, i)$ and $\eta_\delta^l(i, i + 1)$ are both less than α_η and it does not correspond to a big overestimate, or likewise if $\nu_\delta^l(i, i)$ and $\nu_\delta^l(i, i + 1)$ are both greater than $-\alpha_\nu$, then $\Lambda = \Lambda \cup \{i\}$;

- otherwise, if there is a small improvement in the cost function in at least one node using $\hat{\theta}_{\delta, i}^l$, or equivalently the minimum of $\eta_\delta^l(i, :)$ is less than α_η and it does not correspond to a big overestimate, or likewise if $\nu_\delta^l(i, i)$ and $\nu_\delta^l(i, i + 1)$ are both greater than $-\alpha_\nu$, or if there is a change of sign between $\nu_\delta^l(i, i)$ and $\nu_\delta^l(i, i + 1)$, bisect the segment $[x_i^{l+1}, x_{i+1}^{l+1}]$: $\left\{x_1^{l+1}, \dots, x_{n_\theta}^{l+1}\right\} \cup \frac{x_i^{l+1} + x_{i+1}^{l+1}}{2}$. Consider $I = I + 1$ and compute $\hat{\theta}_{\delta, s}^l$, where s represents the indexes of parameters corresponding to the new two subsegments. Then η_δ^l and ν_δ^l are updated considering also those values.

Observe that only $n_\theta - 1$ matrix-vector products are needed in this phase. The choice of the thresholds α_η and α_ν characterized the parametrization: in fact if α_η is chosen too big the algorithm will refine the parameterization less than necessary, whether if it is too small the algorithm will over-refine the parameterization. Instead α_ν is a limit for the allowed overestimation permitted. The optimal choice depends obviously on the specific application, but its tuning is not a problem. Instead, a general auto-tuning strategy is not easy to formulate.

In the corrector step, the projected damped Gauss-Newton method (algorithm 4.1) is applied only to those parameters whose indexes belongs to Λ . Observe that this strategy reduce the ill-conditioning of ψ_θ , since we choose not to optimize parameters which do not improve the value of the cost function, or equivalently parameters whose perturbations do not change significantly the predicted temperatures.

The detailed description of the predictor-corrector is given in algorithm 4.1.

Remark 4.1. Observe that to obtain more reliable estimates, in the predictor step it is better to consider two different perturbation parameters δ_1, δ_2 , and then to consider for every node the minimum value between $\eta_{\delta_1}^l$ and $\eta_{\delta_2}^l$ and between $\nu_{\delta_1}^l$ and $\nu_{\delta_2}^l$ respectively.

5. Numerical results

In this section some numerical experiments are described, to validate the algorithms presented. In particular in (1) and (2) the following values

Algorithm 4.1 Predictor-Corrector algorithm:

-
- 1: Fix a uniform step in $[0, 1]$, $\Delta^0 x$. Consider the coarse subdivision $\{x_1^0, \dots, x_{n_\theta^0}^0\}$,
 $x_1^0 = 0$, $x_i^0 = (i-1)\Delta^0 x$, $x_{n_\theta^0}^0 = 1$, $h_c^0(i) = \Delta^0 x$, $i = 1, \dots, n_\theta^0 - 1$;
 - 2: fix α_η, α_ν , $l = 0$, a small parameter perturbation δ ;
 - 3: $\hat{\theta}^0 = \mathbf{0}_{n_\theta^0 - 1} \in \mathbb{R}^{n_\theta^0 - 1}$;
 - 4: **while** $\mathcal{F}_n(\hat{\theta}^l) \approx \sigma$ **do** { σ is the reference value of the cost function obtained for the sound model }
 - 5: $\left\{x_1^{l+1}, \dots, x_{n_\theta^{l+1}}^{l+1}\right\} = \left\{x_1^l, \dots, x_{n_\theta^l}^l\right\}$, $h_c^{l+1}(i) = h_c^l(i)$, $i = 1, \dots, n_\theta^l - 1$
 - 6: $\Delta^{l+1}x = \frac{\Delta^l x}{2}$, $n_\theta^{l+1} = n_\theta^l$, $I = n_\theta^{l+1} - 1$
 - 7: $\Lambda = \emptyset$, set of indexes of parameters to be optimized
 - 8: **for all** $i \in [1, I]$ **do**
 - 9: compute $\hat{\theta}_{\delta, i}^l$, $\eta_\delta^l(i, :)$ and $\nu_\delta^l(i, :)$
 - 10: **end for**
 - 11: **for all** $i \in [1, I]$ **do**
 - 12: **if** $\max\left\{\eta_\delta^l(i, i), \eta_\delta^l(i, i+1)\right\} < \alpha_\eta$ and $\min\left\{\nu_\delta^l(i, i), \nu_\delta^l(i, i+1)\right\} > -\alpha_\nu$ **then**
 {substantial decrease of the cost function, without overestimating }
 - 13: $\Lambda = \Lambda \cup \{i\}$ % this is a parameter to be optimized
 - 14: $i = i + 1$;
 - 15: **end if**
 - 16: **if** $\min_j\left\{\eta_\delta^l(i, j)\right\} < \alpha_\eta$ and $\min\left\{\nu_\delta^l(i, i), \nu_\delta^l(i, i+1)\right\} > -\alpha_\nu$, or $\nu_\delta^l(i, i) \cdot \nu_\delta^l(i, i+1) < 0$ **then** { moderate decrease of the cost function, without overestimating or change of sign in ν }
 - 17: $n_\theta^{l+1} = n_\theta^{l+1} + 1$, $I = I + 1$; % bisect the corresponding segment
 - 18: $\left\{x_1^{l+1}, \dots, x_{n_\theta^{l+1}}^{l+1}\right\} \cup \frac{x_{i+1}^{l+1} - x_i^{l+1}}{2}$,
 - 19: $h_c^{l+1}(i) = h_c^{l+1}(i+1) = \Delta^{l+1}x$, $h_c^{l+1}(i+2 : \text{end}) = h_c^l(i+1 : \text{end})$,
 - 20: $\eta_\delta^l(i+2 : \text{end}+1, :) = \eta_\delta^l(i+1 : \text{end}, :)$, $\nu_\delta^l(i+2 : \text{end}+1, :) = \nu_\delta^l(i+1 : \text{end}, :)$.
 - 21: **for all** $i \in [i, i+1]$ **do**
 - 22: compute $\hat{\theta}_{\delta, i}^l$, $\eta_\delta^l(i, :)$ and $\nu_\delta^l(i, :)$
 - 23: **end for**
 - 24: **end if**
 - 25: **end for**
 - 26: given the subdivision $\left\{x_1^{l+1}, \dots, x_{n_\theta^{l+1}}^{l+1}\right\}$
 - 27: apply the projected damped Gauss-Newton method, optimizing **only** parameters whose indexes belong to Λ obtaining $\hat{\theta}^{l+1} \in \mathbb{R}^{n_\theta^{l+1} - 1}$
 - 28: $l = l + 1$;
 - 29: **end while**
-

of constants are used: $t_f = 1.51$ s, $L = 0.1$ m; $\rho C = 3.2 \cdot 10^6 \frac{J}{m^3 \circ C}$,

$k = 3.77 \cdot 10^3 \frac{W}{m^{\circ}C}$, and

$$(12) \quad q(t) = \frac{Wt}{\sigma_q^2} e^{-\frac{\sqrt{t}}{\sigma_q}}, \quad t \in (0, t_f]$$

where $\sigma_q = 0.0106$, $W = 2.9511 \cdot 10^{17} J$. The initial condition is set to $T_0(\cdot) = 20^{\circ}C$. In this section an Implicit Euler method is adopted for the time discretization, using a temporal step $\Delta t = 0.0005$ in $(0, 0.1]$ and $\Delta t = 0.05$ in $(0.1, t_f]$. A $P1$ -FE method is used for space discretization, on a variable mesh, whose step length along y is $h_y = 0.01 m$ or $h_y = 0.005 m$, and a variable step along x , depending on the adaptive parametrization. The sensors are supposed to be $n_y = 11$ or $n_y = 21$, distributed with uniform distance $h_x = 0.1 m$ or $h_x = 0.05 m$ respectively. Numerical experiments are carried out using MATLAB.

In all the examples presented, experimental temperatures are simulated numerically. The first step is to validate the numerical model: dealing with pure experimental data, this step is fundamental also to decide the optimal values of the coefficients of the model. In our simulated context, it is still important to estimate the reference minimal value of the cost function σ . To obtain a significative threshold σ , the validation is done using the initial coarse grid used in the estimation of the corroded one. Thus the predictor-corrector strategy reveals uncorroded domains, comparing their cost functions with σ .

In this section the predictor step is applied considering two distinct perturbation parameters, $\delta_1 = 2h_y$ and $\delta_2 = 0.03$ (cfr. Remark 4.1), while the inner-outer strategy builds the sensitivity matrix using a perturbation $\delta = 0.02$.

In Figure 6 the real corroded profiles (left) are compared to the inner-outer (center) and predictor-corrector (right) estimates respectively. As can be seen the predictor strategy tends to refine less and it is also less computationally expensive, due to its linear predictor step. It is important to note that it is formulated such that small overestimates are preferred to underestimates: as a consequence usually the estimated corroded domain is contained in the optimal one, but the distance is small enough. In contrast, although inner-outer algorithm is a simpler strategy, it is more expensive and also tends to over-refine the profile, bisecting also segments which corresponds to null corrosion in the real profile.

In Figure 7, given the real corrosion profile represented in the up-left picture, some iterations of the predictor-corrector algorithm are collected. The algorithm refines properly the segment S : thus ψ_{θ} in the Newton method is computed only for a small subset of parameters, improving its ill-conditioning. Observe that predictor-corrector overestimates only just

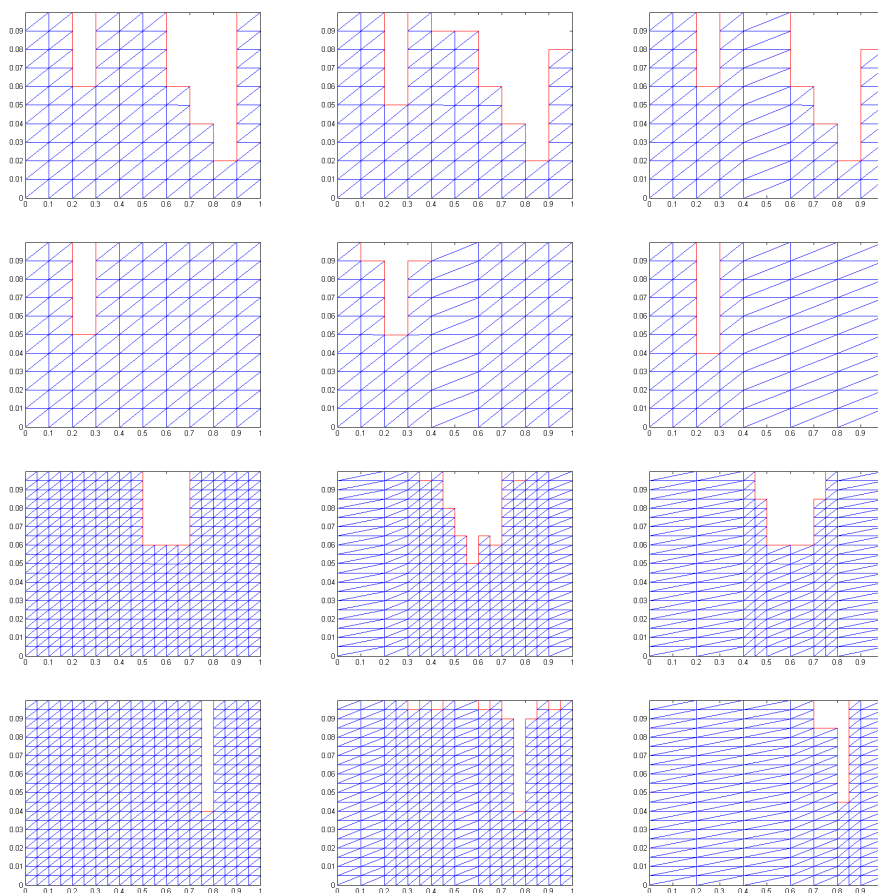


Fig. 6. *Real corroded profiles (left), inner-outer (center) and predictor-corrector (right) estimates.*

outside the corrosion front, due to the diffusive nature of the underlying heat equation. In Figure 8 both the \mathcal{L}^2 -norm of the error (left) and the $O(1)$ estimate of the order of convergence are presented. Thus the adaptive refinement strategy, although it diminishes the computational cost, it causes a slow down in the convergence of a Newton-type algorithm, which is usually $O(2)$, starting near enough to the optimum. Finally observe that, in contrast to the inner-outer algorithm, the predictor-corrector convergence is approximately monotonic, since the refinement of S is entirely done before the local optimization of parameters.

Figure 9 (left) shows a real profile difficult to estimate, due to the presence of two deep corrosion fronts, close to each other. The predictor-

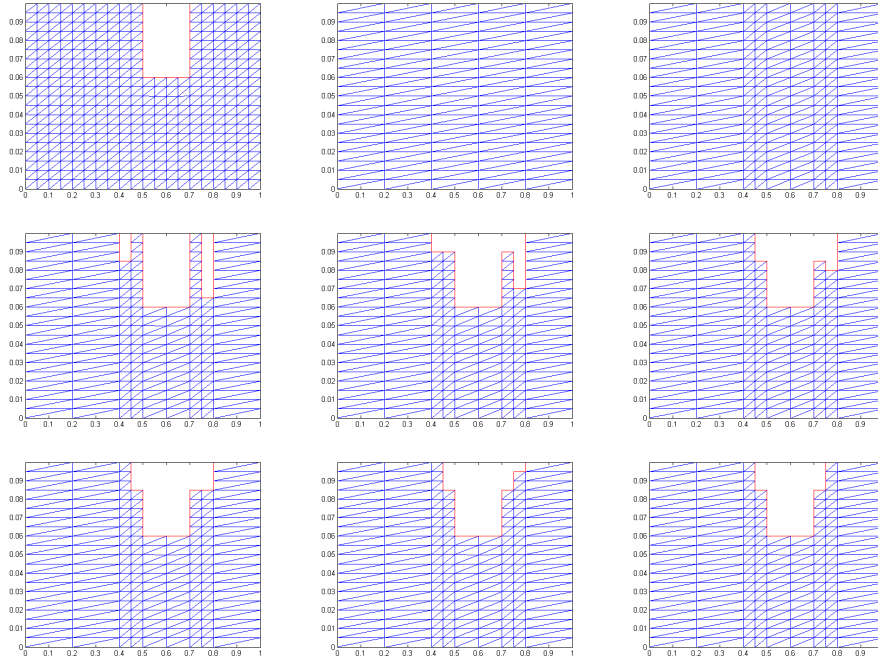


Fig. 7. Real corrosion profile (first row left) and some iterations of the predictor-corrector method.

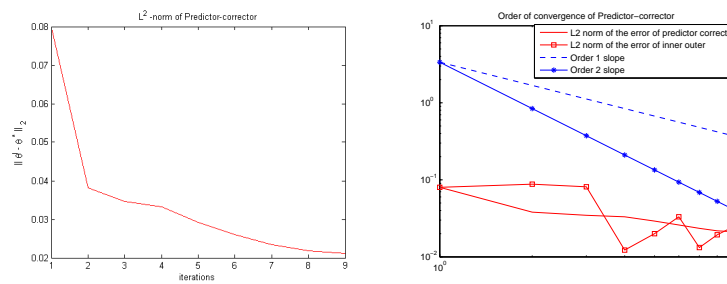


Fig. 8. L^2 -norm of the error and estimates of the order of convergence.

corrector strategy converges to a local minimum (Figure 9 (right)). In fact, as mentioned in section 4.4, the adaptive strategy could introduce local minima in the problem. Observe that inner-outer algorithm could be more robust (Figure 9, center), although it is more computationally expensive. However the estimated predictor-corrector's minimum is a satisfying one, because it reveals both the local position of corrosion and its shape.

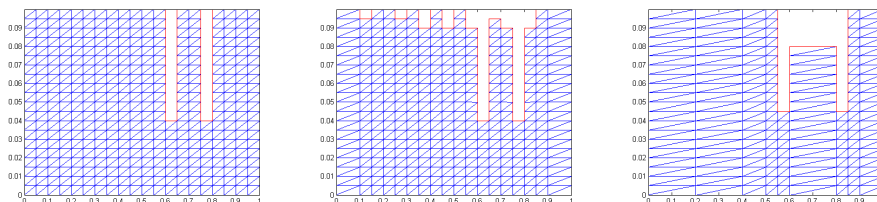


Fig. 9. *Real corrosion profile (left), inner-outer (center) and predictor-corrector (right) estimates.*

6. Conclusions

In this paper a 2D inverse problem of corrosion detection has been presented. Its mathematical formulation suggests to solve it numerically. The numerical approach adopted is based upon an adaptive FE discretization of the heat equation over a variable domain. The inverse problem consists in estimating the vector of parameters that best describes the depth of the real corroded profile. Two algorithms have been presented: Inner-Outer Loop algorithm and Predictor-Corrector algorithm. While the first one is more simple, usually it over-refine S , it is computationally more expensive and corresponds to a worse conditioned problem. The predictor-corrector strategy uses a linear strategy to substitute the outer loop. Moreover it is able to limit the local refinement procedure to proper parts of S , using the norm and the mean of the prediction error. This strategy allows the presence of small overestimates, penalizing huge ones. Due to its linear predictor step and the application of the corrector step only to some selected parameters, it is both less computational expensive and better conditioned. Conducted numerical experiments reveals its ability to refine only where it is necessary and its tendency to obtain small overestimates of the corroded profile.

Acknowledgments

The authors are grateful to P. Mannucci for helpful discussions and her fundamental contribution in the demonstration of Lemma 4.1.

REFERENCES

1. S. Marinetti, P. Bison, and E. Grinzato, 3d heat effects in the experimental evaluation of corrosion by ir thermography, in *Proceedings of the 6th International Conference on Quantitative Infrared Thermography QIRT 2002, Dubrovnik (Croatia)*, pp. 92–98, 2002.

2. V.Vavilov, E.Grinzato, P. Bison, S.Marinetti, and M. Bales, Surface transient temperature inversion for hidden corrosion characterization: Theory and applications, *Int. Journal Heat and Mass Transfer*, vol. 39, pp. 355–371, 1996.
3. P.Bison, D.Fasino, and G.Inglese, Active infrared thermography in non-destructive evaluation of surface corrosion, in *Series on Advances in Mathematics for Applied Sciences - Proceedings of the 7th SIMAI Conference - Venice 2004*, vol. 69, pp. 143–154, World Scientific, 2005.
4. T. Hohage, M. Rapun, and F. Sajas, Detecting corrosion using thermal measurements, *Inverse Problems*, vol. 23, pp. 53–72, 2007.
5. K. Bryan and L. F.Caudill, Uniqueness for a boundary identification problem in thermal imaging, *Electronic Journal of Differential Equations*, vol. 1, pp. 23–39, 1997.
6. K. Bryan and L. F.Caudill, Reconstruction of an unknown boundary portion from cauchy data in n-dimensions, *Inverse Problems*, vol. 21, pp. 239–256, 2005.
7. S.Marinetti and V.Vavilov, Ir thermographic detection and characterization of hidden corrosion in metals: General analysis, *Corrosion Science*, vol. 52, no. 3, pp. 865–872, 2010.
8. L. Ljung, *System Identification: theory for the user*. Prentice Hall, 1987.
9. F. Marcuzzi and S. Marinetti, Efficient reconstruction of corrosion profiles by infrared thermography, *Journal of Physics: Conference Series*, vol. 124, no. 012033, 2008.
10. A. Quarteroni and A. Valli, *Numerical approximation of Partial Differential Equations*. Springer, 1994.
11. A. Quarteroni, *Modellistica numerica per problemi differenziali*. Springer, 2006.
12. A.Friedman, *Partial Differential Equations of Parabolic Type*. Dover Publications, 2008.
13. M.Bertero and P.Boccacci, *Introduction to Inverse problems in imaging*. IOP Publishing Ltd, 1998.
14. H. Engl, M. Hanke, and A. Neubauer, *Regularization of Inverse Problems*. Kluwer, 1996.